Journal of Applied Electrochemistry **33**: 325–331, 2003.

Corrosion behaviour of AB_5-type hydride electrodes in alkaline electrolyte solution

C.S. WANG[1,*], M. MARRERO-CRUZ[1], J.H. BARICUATRO[1], M.P. SORIAGA[1,*], D. SERAFINI[2] and S. SRINIVASAN[3,*]
[1]*Department of Chemistry, Texas A&M University, College Station, TX 77843, USA*
[2]*Department of Physics, Universidad de Santiago de Chile, Santiago, Chile*
[3]*Center for Energy and Environmental Studies, Princeton University, Princeton, NJ 08544, USA*
*(*authors for correspondence)*

Received 19 June 2002; accepted in revised form 4 February 2003

Key words: AB_5-type metal hydride electrodes, corrosion, LaB_5 metal hydride electrodes, $LaNi_{3.35}Co_{0.75}Mn_{0.4}Al_{0.3}$ alloys, Ni-metal hydride electrodes

Abstract

The corrosion rates of $LaNi_5$ and $LaNi_{3.55}Co_{0.75}Mn_{0.4}Al_{0.3}$ hydride electrodes, soaked in alkaline electrolyte and under charge–discharge cycling, were investigated by linear polarization, Tafel polarization and a new method based on the difference between the charge and discharge capacities. The corrosion–inhibition by Ni in $LaNi_5$ and the influence of zincate ions on the corrosion rate of $LaNi_5$ and $LaNi_{3.55}Co_{0.75}Mn_{0.4}Al_{0.3}$ were also studied. The results showed that the hydride electrode exhibits different corrosion behaviour when immersed in alkaline electrolyte and during charge–discharge cycles. The corrosion rate of $LaNi_5$ was lower than that of $LaNi_{3.55}Co_{0.75}Mn_{0.4}Al_{0.3}$ when simply soaked in 6 M KOH solution, but higher during the charge–discharge cycles. The corrosion–inhibition afforded by $Zn(OH)_4^{2-}$ ions on $LaNi_{3.55}Co_{0.75}Mn_{0.4}Al_{0.3}$ is small under quiescent conditions, but increases upon charge–discharge operation; such corrosion–inhibition improves the cycle-life of the hydride electrode.

1. Introduction

It is generally accepted that the corrosion of hydride electrodes not only decreases the hydrogen absorption capability of the electrodes but also the kinetics of the hydriding/dehydriding step [1, 2]. In nickel-metal hydride cells, the Al released by the corroded AB_5 alloy coats the positive electrode and leads to a loss in charging efficiency [3]. Furthermore, since corrosion involves water consumption, the separator ultimately dries out, resulting in an increase in the internal impedance of the cell [4]. The elucidation of the alloy-corrosion mechanism is an important factor in the optimization of the alloy composition of metal-hydride electrode materials.

The electrochemical corrosion of hydride electrodes depends on the pulverization rate of alloys. Alloy decrepitation increases the surface area in contact with the electrolyte, and this increase leads to an enhancement in the corrosion rates [1, 2]. It has been proposed [5] that the magnetic saturation of $MmNi_5$ (where Mm is a Ce-rich rare-earth metal alloy) can be used as an index of the corrosion of such alloys. In alkaline electrolyte, the following oxidation reaction occurs at the reversible hydrogen potential:

$$La(Ni + Co)_3MnAl + 5\ H_2O + 2\ OH^- \longrightarrow La(OH)_3 + 3\ (Ni + Co) + HMnO_2^- + AlO_2^- + 4H_2 \quad (1)$$

In Equation 1, the stoichiometric numbers have been rounded off for simplicity. Ni and Co remain in zerovalent metallic states [5], whereas Al and Mn are dissolved in the alkaline solution [3]. In contrast to Ni and Co, which show ferromagnetism at room temperature, the $LaNi_5$-type alloys exhibit paramagnetic properties [5]. Therefore, the progress of corrosion can be monitored by the variation in magnetic saturation of the alkaline-treated alloy powders [5].

The corrosion rate and corrosion potential of hydrogen-storage alloys in alkaline solution can also be measured by other techniques such as linear polarization, electrochemical impedance spectroscopy and Tafel polarization [6, 7]. However, the use of electrochemical methods for corrosion-rate measurements during charge/discharge cycling is difficult because of interferences from the hydriding/dehydriding process itself. The fact that Al is dissolved from the hydride electrode and becomes completely trapped within the cathode material has led to a suggestion [3] that the Al content at the cathode can be used as an indicator of the degree of alloy corrosion during charge/discharge cycles. Based on

this method the effect of the corrosion of $MmNi_{3.55}Co_{0.75}Mn_{0.4}Al_{0.3}$ on the cell performance of sealed nickel-metal hydride batteries was investigated under charge/discharge operation. However, the Al content of the positive electrode reflects only the corrosion rate of Al and not the over-all corrosion rate of the alloy; moreover, this method is not suitable for Al-free hydride electrodes.

We previously reported that the addition of ZnO to the alkaline electrolyte (to form zincate ions) decreases the corrosion rate of $LaNi_5$-type electrodes. Specifically, extended X-ray absorption fine structure measurements were obtained to demonstrate that zincate ions in the electrolyte inhibit the corrosion of $LaNi_{3.55}Co_{0.75}Mn_{0.4}Al_{0.3}$ electrodes [8,9].

In the present paper, we introduce a new electrochemical method to measure the corrosion rate of hydride electrodes during charge/discharge cycles. This method, along with conventional linear and Tafel polarization measurements, was used to investigate the corrosion of $LaNi_5$ and $LaNi_{3.55}Co_{0.75}Mn_{0.4}Al_{0.3}$ in 6 M KOH solution, with and without addition of 0.5 M ZnO, at a potential range from −0.90 to −0.01 V. At negative potentials, AB_5 alloys are in a hydrided state, whereas, at more positive potentials, the alloys contain no hydrogen. It appears that the new electrochemical method is a versatile and convenient method to evaluate the corrosion of hydride electrodes.

2. Experimental details

2.1. *Preparation of alloy powder and electrode*

Alloy ingots of $LaNi_5$ and $LaNi_{3.55}Co_{0.75}Mn_{0.4}Al_{0.3}$ were prepared by arc-melting a stoichiometrically-proportioned mixture of La, Ni, Co, Mn and Al under a He atmosphere, followed by thermal annealing (at a temperature just below 900 °C) for 72 h. X-ray diffraction (XRD) analysis showed that all the samples were single-phase alloys with a hexagonal $CaCu_5$-type structure. The ingots were then pulverized into a powder (with an average particle-diameter of about 10 μm) by gas-phase hydrogen absorption/desorption cycles. The electrodes were prepared by mixing the alloy powder and binder in a 50:50 weight ratio; the binder used was carbon (Vulcan-XC-72) with 33% polytetrafluoroethylene. This mixture was pressed onto a nickel mesh at a pressure of 300 kg cm^{-2}. The working electrode contained 75 mg of the alloy and had a surface area of about 2 cm^2. A Ni mesh with a surface area 10 times larger than that of the working electrode was used as the counter-electrode. All electrochemical experiments were conducted in a flooded, vented cell that contained 6 M KOH. The potentials were measured with respect to a Hg/HgO reference electrode. Electrochemical measurements made use of an automatic battery cycler (Arbin Corporation, College Station, TX).

2.2. *Corrosion measurement of alloy soaked in alkaline solution*

The open-circuit potential (o.c.p.) was monitored as a function of time while the alloy was immersed in alkaline solution. After the o.c.p. attained a stable value (nominally corresponding to the corrosion potential), the corrosion resistance of the metal-hydride electrode was measured by linear polarization at a sweep rate of 1 mV s^{-1} within a 10 mV overpotential. Potentiodynamic measurements were carried out at the same sweep rate; for the anodic Tafel polarization, the scan was from the established corrosion potential to +0.4 V, whereas, for the cathodic Tafel polarization, the scan was from the corrosion potential to −1.1 V. These polarization measurements were performed using a 273 EG&G PAR potentiostat (Princeton, NJ). The corrosion rate was obtained from Tafel polarization curves, or by linear polarization, using the following equation:

$$I_{\mathrm{corr}} = \frac{\beta_{\mathrm{a}}\beta_{\mathrm{c}}}{2.3(\beta_{\mathrm{a}} + \beta_{\mathrm{c}})R_{\mathrm{c}}} \tag{2}$$

where β_{a} and β_{c} are anodic and cathodic Tafel constants in volts, respectively; R_{c} is the corrosion resistance of the metal-hydride electrode, and I_{corr} is the corrosion rate expressed as current density in mA g^{-1}. In this study, the approximation $\beta_{\mathrm{a}} = \beta_{\mathrm{c}} = 0.1$ V was made when the actual values of the Tafel constants were not known. The error introduced by this approximation is within the experimental scatter of the corrosion measurements [6].

2.3. *Corrosion measurement of activated alloy (between −0.9 V and −0.6 V)*

There are two major steps in the mechanism of alloy corrosion in alkaline solution. At positive corrosion potentials, the following reaction has been suggested to occur on the surface of the hydride electrode [6, 7]:

$$4\,\mathrm{M} + x\mathrm{O}_2 + 2x\mathrm{H}_2\mathrm{O} \longrightarrow 4\,\mathrm{M(OH)}_x \tag{3}$$

Near the reversible hydrogen-evolution potential, the cathodic corrosion reaction is [4, 6]:

$$\left(\frac{1}{x} + \frac{1}{y}\right)\mathrm{M} + \mathrm{H}_2\mathrm{O} \longrightarrow \frac{1}{x}\mathrm{MH}_x + \frac{1}{y}\mathrm{M(OH)}_y \tag{4}$$

Usually, the hydride electrode is charged/discharged in the potential range between −0.6 V and −1.0 V. Therefore, the corrosion of the hydride electrode during charge/discharge cycling is most likely to occur via Equation 4 [4].

There are two other steps related to the generation and desorption of hydrogen during the charge/discharge process. One is the charge/discharge step:

$$\frac{1}{x}\mathrm{M} + \mathrm{H}_2\mathrm{O} + \mathrm{e}^- \longleftrightarrow \frac{1}{x}\mathrm{MH}_x + \mathrm{OH}^- \tag{5}$$

The other step is the self-discharge of the hydride electrode:

$$H_{ad} + H_{ad} \longrightarrow H_2 \quad (6a)$$

or

$$2\,H_{ad} \xrightarrow{\text{dissolved in solution}} 2[H] \xrightarrow{\text{diffusion}} H_2 \quad (6b)$$

If the electrode is cycled at potential ranges below −0.92 V, the self-discharge of the hydride electrode is slow [9], and the electrolytic production of molecular hydrogen when the electrode is charged can be neglected. If hydrogen evolution and alloy oxidation do not occur, and the electrochemical polarization is small, the charge and discharge capacities should be the same after activation. Thus, it is reasonable to estimate the corrosion rate from the difference between the charge and discharge capacities of the metal-hydride electrode at potential ranges below −0.92 V, after the activation process is completed and the capacity remains constant. In fact, the difference between the charge and discharge capacities of the carbon electrode has been successfully used to calculate the rate of formation of a solid–electrolyte interphase film on the carbon anode due to electrolyte reduction (or decomposition) in Li-ion batteries [11].

The corrosion rate, I_{corr}, is defined by the equation:

$$I_{corr} = I_c \times \left(\frac{Q_{disch} - Q_{ch}}{Q_{disch} + Q_{ch}}\right) \quad (7)$$

where I_c is the charge/discharge cycling current in mA g^{-1}; Q_{ch} and Q_{disch} are the charge and discharge capacities, respectively, of the hydride electrodes in mAh g^{-1}.

Electrode activation was performed by charging the electrode with a current of 100 mA g^{-1} for 4 h and then discharging it to −0.6 V at a current of 50 mA g^{-1} for 20 times. The hydrogen evolution due to any overcharge accelerates the activation process. To measure the corrosion rate of the metal-hydride electrode during the activation, a special activation process was used in which the electrode was cycled from −0.9 V to −0.6 V at a charge current of 10 mA g^{-1} and a discharge current of 1 mA g^{-1}. The purpose of using a low charge/discharge current was to increase the absorption of hydrogen into the metal-hydride electrode during the charge process, and then to completely release the hydrogen during the discharge operation.

The corrosion rate of the fully activated metal-hydride electrodes at more negative potentials was measured during 20 cycles of charging/discharging at each of following four potential ranges: −0.91 to −0.88, −0.88 to −0.78, −0.78 to −0.68 and −0.68 to −0.58 V. However, only the average of the charge and discharge capacities from the last five cycles are reported due to the erratic nature of the capacities in the first 15 cycles.

3. Results and discussion

3.1. *Corrosion rate of AB_5 alloys soaked in alkaline solution before activation*

The o.c.p. against time plots for $LaNi_5$ and $LaNi_{3.55}Co_{0.75}Mn_{0.4}Al_{0.3}$ soaked in 6 M KOH solution, with and without ZnO, are displayed in Figure 1. Also shown for comparison, is the o.c.p. of a 'blank' electrode composed only of the binding materials and Ni mesh. For a carbon–nickel electrode, a nearly-constant o.c.p., with only a very slow drift toward more positive potentials, was observed; this is presumably due to the stability of carbon and the passivation of Ni at potentials more positive than −0.5 V [12]. The same constancy in the o.c.p. of the $LaNi_5$ electrode was found, with a value slightly higher (by 0.04 V) than that of the carbon–nickel electrode. Thus, the corrosion behaviour of $LaNi_5$ soaked in 6 M KOH is similar to that of Ni. However, a different behaviour in the o.c.p. of $LaNi_{3.55}Co_{0.75}Mn_{0.4}Al_{0.3}$ electrode was observed. Initially, the o.c.p. of the $LaNi_{3.55}Co_{0.75}Mn_{0.4}Al_{0.3}$ electrode shifted towards the positive direction; it then plummeted to negative values before it finally remained invariant at a potential of about −0.7 V. When the immersion time was increased further, the potential drifted again in the positive direction.

The data in Figure 1 can be explained by taking into account the passivation and dissolution processes that affect the electrode surface. Before immersion, a thin layer of oxide, such as La_2O_3 and NiO, covers the $LaNi_5$ and $LaNi_{3.55}Co_{0.75}Mn_{0.4}Al_{0.3}$ electrodes. Upon immersion, $La(OH)_3$ is formed at potentials below 0.1 V in pH 14–16 solution [12]; on the other hand, a $Ni(OH)_2$ (or Ni_3O_4) film prevents further oxidation of Ni. Consequently, $LaNi_5$ shows a lower corrosion rate in 6

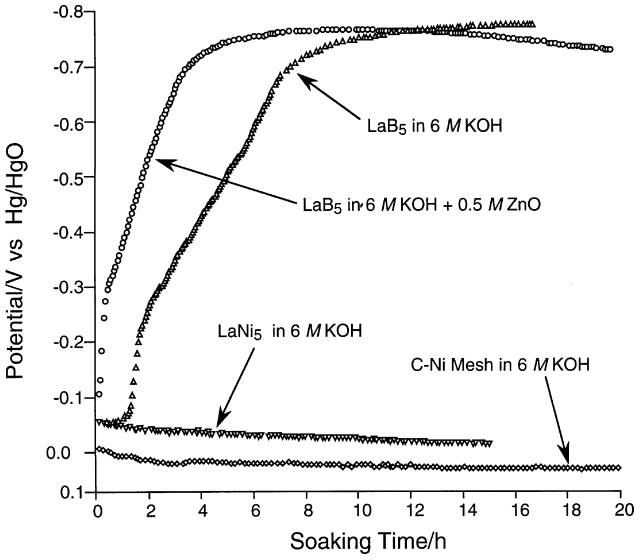

Fig. 1. Plots of open-circuit potential (o.c.p.) as a function of time for $LaNi_5$ and $LaNi_{3.55}Co_{0.75}Mn_{0.4}Al_{0.3}$ in 6 M KOH solution with and without 0.5 M $Zn(OH)_4^{2-}$ before activation. The o.c.p. of a 'blank' electrode composed only of the binding materials and Ni mesh is also shown in Figure 1 for comparison.

M KOH solution. As expected, the Tafel polarization (Figure 2) and linear polarization data showed that the corrosion rate of $LaNi_5$ is only about 0.11 mA g^{-1} at −0.03 V and 0.09 mA g^{-1} at 0.0 V (Table 1). Also from Figure 2, it can be seen that, at a high cathodic polarization, a limiting current representing an oxygen diffusion-controlled process arises. These findings are consistent with published results [7]. It can thus be assumed that, at the corrosion potential, Equation 3 occurs at the surface of the $LaNi_5$ electrode.

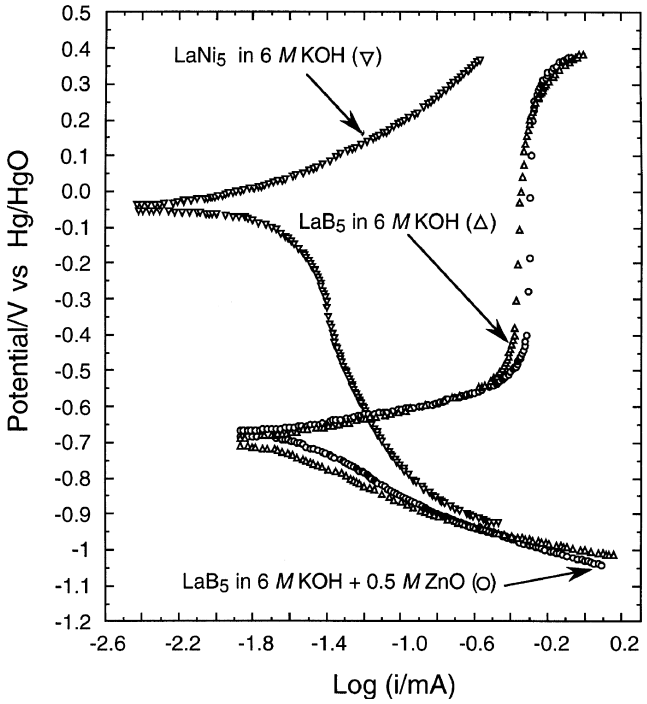

Fig. 2. Potentiodynamic polarization curves for $LaNi_5$ and $LaNi_{3.55}Co_{0.75}Mn_{0.4}Al_{0.3}$ in 6 M KOH solution with and without 0.5 M $Zn(OH)_4^{2-}$ before activation.

Table 1. Corrosion rates and exchange currents of AB_5 alloys

Alloys	*E* /V	I_{corr} in 6 M KOH /mA g^{-1}	I_{corr} in 6 M KOH + 0.5 M $Zn(OH)_4^{2-}$ /mA g^{-1}
Before activation			
$LaNi_{3.55}Co_{0.75}Mn_{0.4}Al_{0.3}$	−0.7	0.42	0.4
	−0.68	0.4	0.38
	−0.6	0.38	0.35
	−0.5	0.35	0.34
	−0.4	0.32	
	−0.27	0.3	0.3
$LaNi_5$	−0.03	0.11	
	0	0.09	
After activation			
$LaNi_{3.55}Co_{0.75}Mn_{0.4}Al_{0.3}$	−0.9	70*	72*
	−0.88	44*	44*
	−0.78	35*	36*
	−0.63	9.5*	9*
	−0.58	4	3.8
	−0.01	1.3	1.2
$LaNi_5$	−0.2	1.2	
	−0.1	0.89	

*Data calculated from Equation 8. Other values calculated from Equation 2.

The solubility, in alkaline solution, of the Mn and Al oxide films in $LaNi_{3.55}Co_{0.75}Mn_{0.4}Al_{0.3}$ [3] results in a gradual increase in the corrosion rate. When the anodic oxidation current for the corrosion of $LaNi_{3.55}Co_{0.75}Mn_{0.4}Al_{0.3}$ increases faster than the cathodic reduction current, the o.c.p. of the electrode becomes more negative than that of $LaNi_5$. In this study, at a potential of −0.76 V, the anodic current became equal to the cathodic reduction, and a stable potential was reached. As the thickness of the surface oxide increased, the anodic current decreased; as a result, the potential shifted to more positive values. Unlike the Tafel polarization of $LaNi_5$, $LaNi_{3.55}Co_{0.75}Mn_{0.4}Al_{0.3}$ did not exhibit a cathodic limiting current, as can be seen in Figure 2. Therefore, the cathodic reaction switched from Equation 3 to Equation 4. The observed corrosion behaviour of $LaNi_{3.55}Co_{0.75}Mn_{0.4}Al_{0.3}$ soaked in alkaline solution corroborates published data [4]. Moreover, hydrogen is believed to be stored in $LaNi_{3.55}Co_{0.75}Mn_{0.4}Al_{0.3}$ because such electrode can deliver about 0.5 mAh g^{-1} at a corrosion potential of −0.75 V.

The presence of $Zn(OH)_4^{2-}$ ions did not markedly affect the corrosion potential of $LaNi_{3.55}Co_{0.75}Mn_{0.4}Al_{0.3}$ (Figure 2), but it slightly decreased the corrosion rate (Table 1). The present results show that the $LaNi_5$ alloy has a higher anticorrosion ability than $LaNi_{3.55}Co_{0.75}Mn_{0.4}Al_{0.3}$ when both alloys are soaked in 6 M KOH solution before activation.

3.2. *Corrosion rate of AB_5 alloys during the activation process in 6 M KOH solution*

During charge/discharge cycles, the AB_5 particles become pulverized. Such pulverization is brought about by the large volume differences between the metallic and hydride phases. Newly generated surfaces are exposed to the alkaline solution and, hence, the corrosion rate is enhanced.

Figure 3 shows the charge and discharge capacities at a potential range from −0.9 to −0.6 V with a charge current of 10 mA g^{-1} and a discharge current of 1 mA g^{-1}; both capacities were similar within the first few charge/discharge cycles. However, upon electrode activation, the discharge capacity became gradually higher than the charge capacity; this implies that the corrosion rate increases rapidly during the activation process. The observed experimental trend demonstrates that the new method is capable of monitoring the corrosion of the hydride electrode during charge/discharge cycles.

3.3. *Corrosion rate of AB_5 alloys in alkaline solution after activation*

During alkaline soaking, the potential of the fully activated $LaNi_{3.55}Co_{0.75}Mn_{0.4}Al_{0.3}$ and $LaNi_5$ electrodes

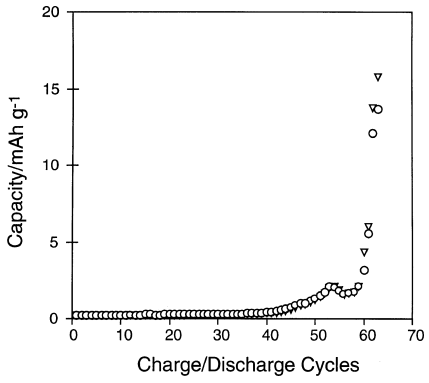

Fig. 3. Charge and discharge capacities of $LaNi_{3.55}Co_{0.75}Mn_{0.4}Al_{0.3}$ electrode during activation. Charge current: 10 mA g^{-1}; discharge current: 1 mA g^{-1}; cycling potential range: −0.9 to −0.6 V vs. Hg/HgO. Key: (○) charge; (▽) discharge.

shifted in the positive direction. It is reasonable to suppose that, at potentials more positive than −0.6 V, at which the alloy contains no hydrogen, the electrochemical corrosion of the alloy is the principal step. Therefore, the corrosion current can be determined from Equation 2. The results are shown in Table 1. The post-activation corrosion rate of $LaNi_5$ and $LaNi_{3.55}Co_{0.75}Mn_{0.4}Al_{0.3}$ was faster than that prior to activation because of surface area enhancement associated with the pulverization of AB_5 alloys.

At potentials more negative than −0.6 V, at which the alloy contains hydrogen, the hydrogen charging/discharging process is the main reaction; hence, Equation 2 can no longer be used to calculate the corrosion rate of the alloy at such potential range. In fact, the resistance (R_{ct}), determined from linear polarization in the potential range from −0.9 to −0.6 V, reflects the charge-transfer resistance due to hydrogen absorption/desorption and to alloy corrosion. At potentials more negative than −0.6 V, the current calculated from Equation 8,

$$I_o = \frac{RT}{FR_{ct}} = \frac{0.0257}{R_{ct}} \tag{8}$$

is actually the exchange current (I_o) due to hydrogen absorption/desorption and alloy corrosion. The results are shown in Table 1. The post-activation corrosion rate of $LaNi_5$ and $LaNi_{3.55}Co_{0.75}Mn_{0.4}Al_{0.3}$ at potentials more positive than −0.6 V was faster than that before activation because of surface-area enhancement associated with the pulverization of AB_5 alloys.

To eliminate the influence of the hydrogen charge/discharge current on the corrosion rate of fully activated metal-hydride electrodes at potentials more negative than −0.6 V, Equation 7, which is based on the difference between charge and discharge capacities, was used to calculate the corrosion rate. Measurements were performed for four different potential ranges: −0.91 to −0.88 V, −0.88 to −0.78 V, −0.78 to −0.68 V, and −0.68 to −0.58 V. Potentials more negative than −0.91 V were avoided to limit the evolution of hydrogen gas. The chosen upper limit of −0.58 V corresponds to the cut-off potential typically used during electrode testing. When the electrode was cycled between −0.91 to −0.88 V, the corrosion rate approached zero. The difference between the charge and discharge capacities reflects the corrosion behaviour of the hydride phase. For a given potential range, the reported corrosion rate was defined as the rate obtained at the median of the potential range.

To measure the corrosion rate more accurately, the effect of the charge/discharge current on the corrosion rate was firstly investigated. The results are shown in Figure 4. The cycling current had no obvious influence on the corrosion rate: the corrosion rate measured at a current of 50 mA g^{-1} was only slightly higher than that measured at 25 mA g^{-1}. This small difference can be attributed to the short measurement time at the current of 50 mA g^{-1} that served to decrease the hydrogen evolution rate. When the cycling current exceeded 100 mA g^{-1}, the electrochemical polarization increased rapidly, and charge and discharge capacities became erratic; the corrosion-rate measurement was thus rendered inaccurate and imprecise. A cycling current of 50 mA g^{-1} was therefore used during the measurement of the corrosion rates. In Figure 4, the decrease in corrosion rate when the potential-cycling range was shifted in the negative direction is due to the high anticorrosion ability of the hydride phase. This result is in agreement with the fact that the cycle-life of hydride electrodes increases as the extent of discharge decreases. The low corrosion rate of the metal-hydride at high hydrogen content is primarily due to the facts that: (i) at more negative potential, the corrosion of alloy becomes slow, and (ii) the oxidation rate of hydrogen stored in the metal-hydride is faster than the corrosion of the alloy which results in cathodic protection.

Figure 5 shows the corrosion rate of $LaNi_5$ and $LaNi_{3.55}Co_{0.75}Mn_{0.4}Al_{0.3}$ measured at identical charge and discharge currents of 50 mA g^{-1}. Before activation, the corrosion rate of $LaNi_5$ was lower than that of $LaNi_5C_{0.75}Mn_{0.4}Al_{0.3}$. However, the reverse was observed for a fully activated $LaNi_5$. A possible explanation for this reversal is the higher pulverization rate of

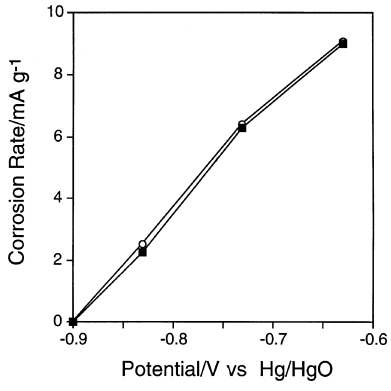

Fig. 4. Corrosion rate of the activated $LaNi_{3.55}Co_{0.75}Mn_{0.4}Al_{0.3}$ electrode measured at different charge/discharge currents: (○) 50 mA g^{-1}; (■) 25 mA g^{-1}.

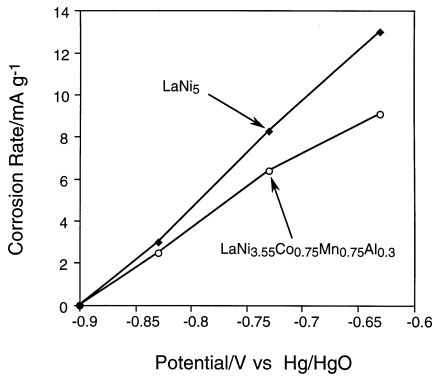

Fig. 5. Effect of Ni substitution on the corrosion rate of the activated $LaNi_5$ in 6 M KOH solution.

$LaNi_5$ relative to that of $LaNi_{3.55}Co_{0.75}Mn_{0.4}Al_{0.3}$. In other words, the corrosion behaviour of hydrogen-storage alloys measured only while soaked in alkaline solution, does not reflect the true corrosion rate during charge/discharge cycling.

3.4. *Corrosion rate of fully activated $LaNi_{3.55}Co_{0.75}Mn_{0.4}Al_{03}$ in the potential range −0.9 to −0.01 V*

The corrosion rate of fully activated $LaNi_{3.55}Co_{0.75}Mn_{0.4}Al_{0.3}$ in the potential range −0.9 to −0.01 V is shown in Figure 6; for comparative purposes, the exchange currents due to hydrogen absorption/desorption and alloy corrosion at potentials more negative than −0.6 V are also shown. At potentials more negative than −0.6 V, the corrosion rates were obtained from the difference between the charge and discharge capacities using Equation 7. At potentials more positive than −0.6 V, the rates were calculated from linear and Tafel polarization using Equation 2.

From Figure 6 it can be seen that the exchange current measured from linear polarization decreased while the corrosion rate increased as the potential was scanned to more positive values. The two curves intersected at a potential of about −0.6 V, implying that, below −0.6 V, the current density measured from linear polarization reflected the corrosion rate. Figure 6 confirmed that the reaction resistance determined from linear polarization does not only encompass contributions from the electrochemical hydrogen absorption/desorption reaction resistance [13], but also includes the corrosion resistance of the alloy, especially at more positive potentials.

3.5. *Effect of $Zn(OH)_4^{2-}$ on corrosion behaviour*

Previous X-ray absorption near-edge spectroscopy (XANES) studies showed that $Zn(OH)_4^{2-}$ present in 6 M KOH solution can improve the cycle life of $LaNi_{3.55}Co_{0.75}Mn_{0.4}Al_{0.3}$ due to a significant lowering of the buildup rate of $Ni(OH)_2$ in the alloys [8]. From the XANES results, it can be inferred that the improvement in the cycle life is due to corrosion inhibition. Figure 7 shows the corrosion behaviour of a fully activated $LaNi_{3.55}Co_{0.75}Mn_{0.4}Al_{0.3}$ electrode in 6 M KOH solution with and without 0.5 M $Zn(OH)_4^{2-}$ measured using Equation 7. The present results confirmed that the presence of $Zn(OH)_4^{2-}$ retards the corrosion rate. The protective effect of $Zn(OH)_4^{2-}$ is dominant during cycling but is not pronounced during simple soaking. This difference in behaviour stems from the fact that Zn is more readily electrodeposited onto the $LaNi_{3.55}Co_{0.75}Mn_{0.4}Al_{0.3}$ alloy during cycling at potentials below −0.75 V. X-ray photoelectron spectroscopy measurements of post-cycled $LaNi_{3.55}Co_{0.75}Mn_{0.4}Al_{0.3}$ alloy, along with results obtained from inductively coupled plasma-optimal emission spectroscopic analysis of the spent solution, revealed that Zn is underpotentially deposited from solution onto the alloy during the charge/discharge cycles [9].

4. Conclusions

The corrosion behaviour of AB_5-type alloy electrodes in alkaline solution has been investigated by linear polarization, Tafel polarization, and a new galvanostatic charge/discharge method. The results showed that the corrosion rate of AB_5-type hydride electrode during

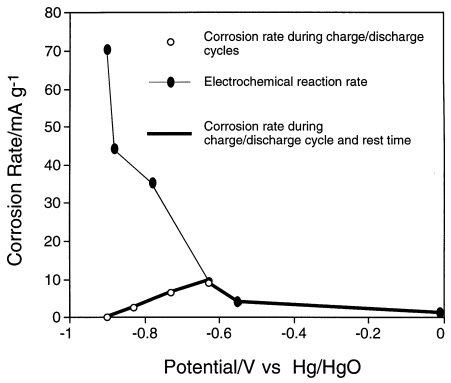

Fig. 6. Corrosion rate of fully activated $LaNi_{3.55}Co_{0.75}Mn_{0.4}Al_{0.3}$ electrode in the potential range −0.9 to −0.01 V.

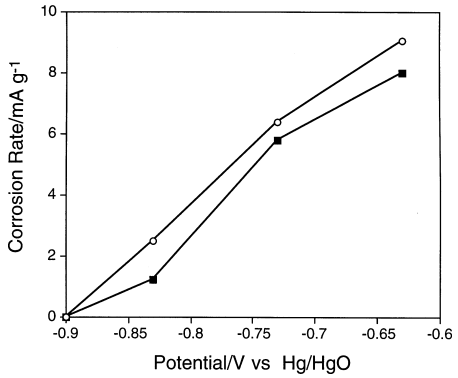

Fig. 7. Effect of $Zn(OH)_4^{2-}$ present in 6 M KOH solution on the corrosion rate of the activated $LaNi_{3.55}Co_{0.75}Mn_{0.4}Al_{0.3}$ electrode. Key: (○) 6 M KOH; (■) 6 M KOH + 0.5 M ZnO.

charge/discharge cycles can be measured from the difference between the capacity upon charging and that upon discharging. The corrosion rate of the $LaNi_5$ and $LaNi_{3.55}Co_{0.75}Mn_{0.4}Al_{0.3}$ electrodes increased almost linearly as the potential was swept toward more positive values. The corrosion rate of $LaNi_5$ was smaller than that of $LaNi_{3.55}Co_{0.75}Mn_{0.4}Al_{0.3}$ electrodes when simply immersed, but the reverse was noted after several charge/discharge cycles. The corrosion rate of the hydride electrodes simply soaked in alkaline solution does not reveal the real corrosion behaviour during charge/discharge cycles. $Zn(OH)_4^{2-}$ ions present in the electrolytic solution inhibited the corrosion rate of $LaNi_{3.55}Co_{0.75}Mn_{0.4}Al_{0.3}$ electrodes during the charge/discharge cycles.

Acknowledgements

The work was performed under the auspices of the US Department of Energy, Division of Chemical Sciences, Office of Basic Energy Science (Contract DE-FG03-93ER1481).

References

1. C.S. Wang, Y.Q. Lei and Q.D. Wang, *Electrochim. Acta* **43** (1998) 3193.
2. C.S. Wang, Y.Q. Lei and Q.D. Wang, *Electrochim. Acta* **43** (1998) 3209.
3. P. Bernard, *J. Electrochem. Soc.* **145** (1998) 456.
4. P. Leblanc, C. Jordy, B. Knosp and Ph. Blanchard, *J. Electrochem. Soc.* **145** (1998) 860.
5. M. Yamamoto and M. Kanda, *J. Alloy. Compd.* **253** (1997) 660.
6. D.A. Jones. 'Principles and Prevention of Corrosion' (Lehigh Press, New York, 1992).
7. M.P.S. Kumar, W. Zhang, K. Petrov, A.A. Rostami, S. Srinivasan, G.D. Adzic, J.R. Johnson, J.J. Reilly and H.S. Lim, *J. Electrochem. Soc.* **142** (1995) 3424.
8. L.S. Mukerijee, J. McBreen, C. Adzic, J.R. Johnson, J.J. Reilly, M.R. Marrero, M.P. Soriaga, M.S. Alexander, A. Visitin and S. Srinivasan, *J. Electrochem. Soc.* **144** (1997) L258.
9. C.S. Wang, M.M. Cruz, M.P. Soriaga, D. Serafini and S. Srinivasan, *Electrochim. Acta* **47** (2002) 1069.
10. C.S. Wang, X.H. Wang, Y.Q. Lei, C.P. Chen and Q.D. Wang, *Int. J. Hydrogen Energy* **22** (1997) 1117.
11. C.S. Wang, A.J. Appleby and F.E. Little, *J. Electroanal. Chem.* **519** (2002) 9.
12. M. Pourbaix, 'Atlas of Electrochemical Aqueous Solutions' (J.W. Arrowsmih Ltd, Bristol, 1966).
13. C.S. Wang, M.P. Soriaga and S. Srinivasan, *J. Power Sources* **85** (2000) 212.